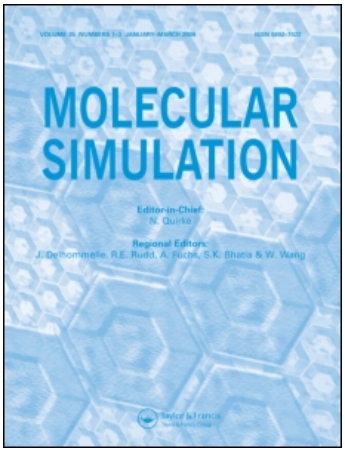

Molecular Simulation
Publication details, including instructions for authors and subscription information:
http://www.informaworld.com/smpp/title~content=t713644482

Geometrical deformation and failure behavior of C_{60} fullerene dimer under applied external electric field

H. Shen[a]
[a] School of Aeronautics and Astronautics, Nanjing University of Aeronautics & Astronautics, Nanjing, P.R. China

To cite this Article Shen, H.(2006) 'Geometrical deformation and failure behavior of C_{60} fullerene dimer under applied external electric field', Molecular Simulation, 32: 1, 59 — 64
To link to this Article: DOI: 10.1080/08927020600582804
URL: http://dx.doi.org/10.1080/08927020600582804

Molecular Simulation, Vol. 32, No. 1, 15 January 2006, 59–64

Taylor & Francis
Taylor & Francis Group

Geometrical deformation and failure behavior of C_{60} fullerene dimer under applied external electric field

H. SHEN*

School of Aeronautics and Astronautics, Nanjing University of Aeronautics & Astronautics, Nanjing 210016, P.R. China

(Received December 2005; in final form January 2006)

By the quantum-molecular dynamics (QMD) technique based on the Roothaan–Hall equation and the Newton motion law, geometrical deformation and failure behavior of C_{60} fullerene dimer ($2C_{60}$) as well as single C_{60} fullerene under applied external electric field are simulated. Further, the effects of the electric field direction on the electric field-induced deformation, polarization-charge distribution and dipole moment of the fullerene molecules are discussed systemically. It is found that the geometrical configuration and failure behavior of the $2C_{60}$ molecule are sensitive to the electric field direction, that when the electric field direction is parallel to the bridging C–C bonds of the $2C_{60}$ molecule the $2C_{60}$ fails easily, and that when the electric field direction is perpendicular to the $2C_{60}$ fails difficultly and has the same polarization and failure mechanism as the single C_{60}.

Keywords: C_{60} dimer; Fullerene; Geometry configuration; Failure; External electric field

1. Introduction

Carbon fullerene, a novel form of carbon first discovered in 1985 [1], has been recognized as important nanoscopic system [2]. Due to its exceptional electric, optical and mechanical properties, carbon fullerene, especially the most common C_{60} fullerene, has been attracting scholars' attention [2–6]. In 1994, chain-like C_{60} polymers were also found by Pekker *et al.* [5]. Among the polymers, the simplest C_{60} dimer ($2C_{60}$) was proved to have excellent electric and optical properties [7,8]. However, up to now there is little report on the electric field-induced failure of the $2C_{60}$.

Considering the above reason, in this paper, the quantum-molecular dynamics (QMD) technique based on the Roothaan–Hall equation and the Newton motion law is used to calculate the deformation, polarization-charge distribution and molecular dipole moment of the C_{60} dimer under the external electric-field with different intensity and direction. For comparison, the similar simulation is also performed to one single C_{60} fullerene. At last, according to the computed results, the geometrical configuration and failure behavior of the $2C_{60}$ and C_{60} molecule are discussed. Some interesting conclusions are given in the present paper, which are very valuable for people to cognize the physical properties of the C_{60} dimer.

2. Model

2.1 The investigated objects

Figure 1 shows the C_{60} dimer to investigate. The dumb-bell-shaped molecule has two C_{60} fullerenes, the two fullerenes are bridged each other through a pair of parallel C–C bonds (called as "bridging C–C bonds" here) and each C_{60} fullerene sphere consists of 12 regular pentagon and 20 regular hexagon faces. The external electric field is applied in the direction of the *x*-, *y*- or *z*-axis, and the electric field intensity E_e takes between 0 and 0.13 au. For the convenience of comparison, the electric field-induced deformation and failure of the single C_{60} fullerene is simulated as well. The initial diameter d_0 of both the single C_{60} fullerene and the C_{60} fullerenes of the $2C_{60}$ molecule is of about 0.71 nm, and the initial length l_0 of the bridging C–C bonds of the $2C_{60}$ is of about 0.15 nm.

2.2 The QMD method

In the present paper, the QMD technique [9] is used to simulate the electric field-induced deformation and failure of the $2C_{60}$ and C_{60} molecule. In the simulation technique, the positions and velocities of the carbon atoms in the

* Corresponding author. Email: shj@nuaa.edu.cn

Molecular Simulation
ISSN 0892-7022 print/ISSN 1029-0435 online © 2006 Taylor & Francis
http://www.tandf.co.uk/journals
DOI: 10.1080/08927020600582804

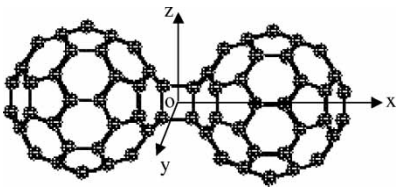

Figure 1. The C_{60} fullerene dimer.

$2C_{60}$ or C_{60} molecule are predicted with Newton's equation:

$$\ddot{r}_i = \frac{F_i(r_i)}{m_i} \tag{1}$$

$$F_i = -\frac{\partial E}{\partial r_i} \tag{2}$$

where $\ddot{r}_i$, r_i, F_i and m_i are the acceleration, coordinates, resultant force and mass of the ith carbon atom, respectively. The molecular energy E in equation (2) is determined by the Schrödinger equation:

$$\mathbf{H}\Psi = E\Psi \tag{3}$$

where $\mathbf{H} = \mathbf{H}_0 + V(r)$. $\mathbf{H}_0$ is the Hamilton operator of the molecular systems, $V(r)$ the electric potential of the external electric field and Ψ the wave function of the $2C_{60}$ or C_{60} system.

In fact, it is difficult to strictly solve any multi-atomic system by the above Schrödinger equation. Accordingly, the Born-Oppenheimer assumption, by which the motion of electrons and nuclei can be decoupled, and the Hartree–Fock assumption, by which the multi-atomic problem in equation (3) can be simplified into a single-electronic problem, are often used so that equation (3) can be approximately replaced by the Hartree–Fock equation below:

$$\mathbf{H}_i\Psi_i = \varepsilon_i\Psi_i \tag{4}$$

where $\mathbf{H}_i$ is the effective single-electronic Hamilton operator, Ψ_i the ith molecular orbital (MO) and ε_i the energy of the MO Ψ_i.

When the assumption of the linear combination of atomic orbitals (LCAO) is used,

$$\Psi_i = \sum_{\mu} C_{\mu i}\Phi_{\mu},$$

in which $\Phi_{\mu i}$ is the μth atomic orbital (AO) and $C_{\mu i}$ the coefficient corresponding to the AO $\Phi_{\mu i}$.

By means of the close-shell model and the restricted Hartree–Fock method (RHF method) [10], equation (4) can be translated into the following matrix form, i.e. the Roothaan–Hall equation [11]:

$$\mathbf{FC} = \mathbf{SCE} \tag{5}$$

Where, **F** represents the Fock matrix, **S** the overlapping integrals matrix, **C** the coefficient matrix and **E** the orbital diagonal energy matrix. Using the self-consistent field (SCF) method, we can solve equation (5) to obtain the molecular energy E.

In [9], the semi-empirical PM3 QM method [10] is used to investigate the electric field-induced failure of carbon nanotubes. Considering the calculation efficiency, the semi-empirical QM method is also adopted here. All the pre-, post-processes and computations are carried out in the quantum-chemical software of Hyperchem 7® [12]. In the simulations, the time-step for MD calculations takes 0.001 ps and the convergence limit 0.01 kcal/mol.

3. Results and discussion

Figure 2 presents the molecular configurations of the $2C_{60}$ under the x-axis electric field with different intensity. In the figures, the polarization-charge on each

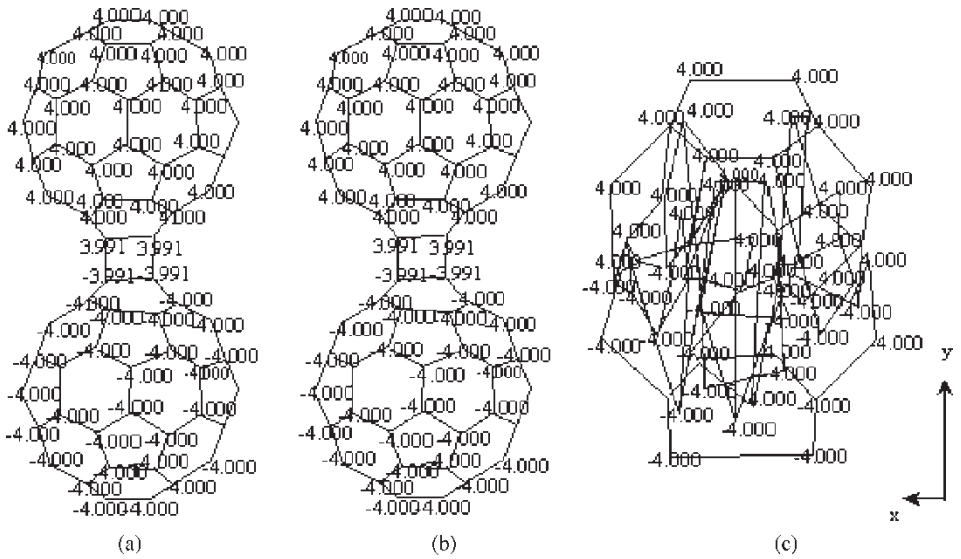

Figure 2. The $2C_{60}$ under the x-axis electric field with the intensity of: (a) 0.01 au, (b) 0.02 au and (c) 0.022 au.

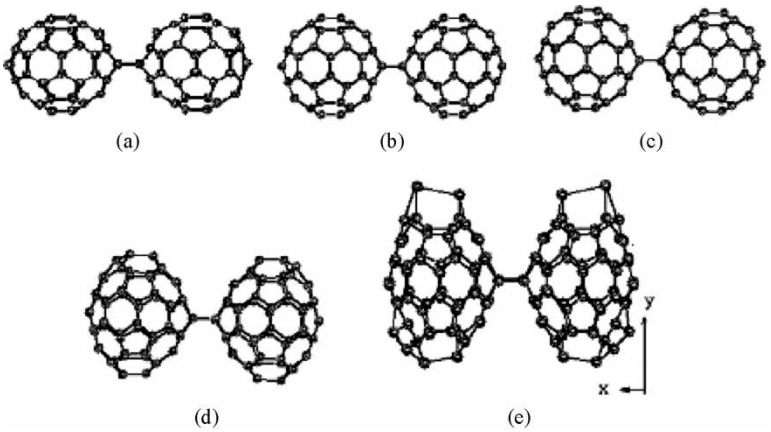

Figure 3. The $2C_{60}$ under the y-axis electric field with the intensity of: (a) 0 au, (b) 0.05 au, (c) 0.075 au, (d) 0.10 au and (e) 0.125 au.

carbon atom is marked. The unit of the net-charge is elementary electronic charge. Figures 3 and 4 show the molecular configurations of the $2C_{60}$ under the y- and z-axis electric field, respectively. Figure 5 presents the configurations of the single C_{60} under electric field. Figure 6 shows the polarization-charge distribution of the $2C_{60}$ molecule under the y-axis electric field with different intensity. The charge distribution and electronic density of the $2C_{60}$ molecule under z-axis electric field, as well as the single C_{60} molecule under electric field, are similar to the cases in figure 6, so they are not shown here. Figure 7 presents the change of the diameter d of the single C_{60} and the C_{60} of the $2C_{60}$ molecule under electric field, where the d refers to the diameter parallel to the electric field direction. In figure 7, the change of the length l of the bridging C−C bonds in the $2C_{60}$ under the x-, y- and z-axis electric field is shown as well.

According to figures 2−7, it can be found that:

(1) The geometrical evolvement of the C_{60} fullerenes of the $2C_{60}$ molecule under the y- and z-axis electric field is similar to that of the single C_{60} under electric field. When the applied electric field intensity $E_e < 0.05$ au, both the single C_{60} and the C_{60} of the $2C_{60}$ molecule are slightly elongated along the electric field direction, and when the $E_e > 0.05$ au, they are elongated markedly and become ellipsoids. Their maximal elongation $(d/d_0)_{max}$ along the electric field direction can even reach 152 ∼ 162% before they fail. The $(d/d_0)_{max}$ values are listed in table 1. When the E_e increases to certain critical value E_c, the single C_{60} and the C_{60} of the $2C_{60}$ molecule fail and some of their C−C bonds are broken as shown in figures 3−5(e). The critical E_c values are tabulated in table 1 as well.

(2) The geometrical evolvement and failure behavior of the $2C_{60}$ under the x-axis electric field is apparently different from those of the single C_{60} as well as the $2C_{60}$ under the y- and z-axis electric field. First, the critical intensity E_c of the x-axis electric field, under which the $2C_{60}$ molecule fails, is very small, and only about 0.021 au. Secondly, contrary to what we expected, two bridging C−C bonds of the $2C_{60}$ molecule do not break under the x-axis electric field, and the two C_{60} fullerenes collide into each other when the $E_e \approx E_c$ and become into a cocoon-like C_{120} atomic-cluster as shown in figure 4(c). Thirdly, the $2C_{60}$ under the x-axis electric field has the $(d/d_0)_{max}$ about only 108%, which is much less than those of the single C_{60} and the $2C_{60}$ molecule under the y- and z-axis electric field. The $(d/d_0)_{max}$ values of the single C_{60} and the $2C_{60}$ molecule under the y-

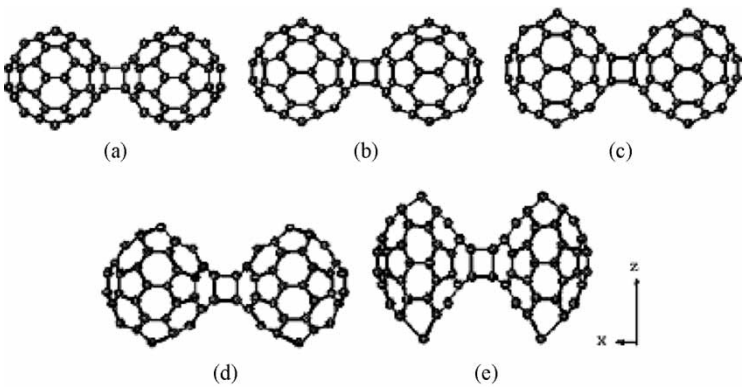

Figure 4. The $2C_{60}$ under the z-axis electric field with the intensity of: (a) 0 au, (b) 0.05 au, (c) 0.075 au, (d) 0.10 au and (e) 0.125 au.

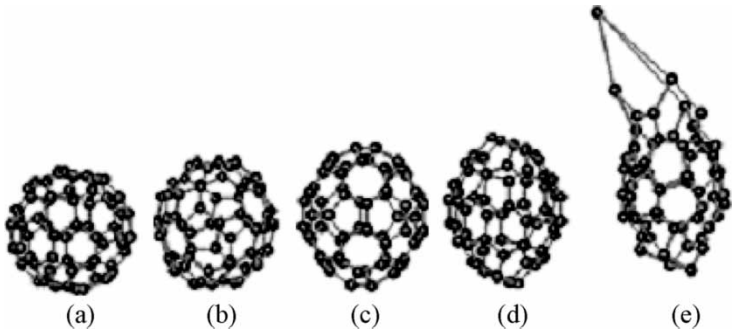

Figure 5. The C_{60} molecule under the electric field with the intensity of: (a) 0.0 au, (b) 0.025 au, (c) 0.05 au, (d) 0.075 au and (e) 0.125 au.

and z-axis electric field are 152, 158 and 162%, respectively (see table 1).

(3) Under the y- and z-axis electric field, the two C_{60} fullerenes of the $2C_{60}$ molecule have negative polarization-charge on their carbon atoms close to the anode of the external electric field, and have positive charge on those close to the cathode (see figure 6). Under the x-axis electric field, the entire C_{60} of the $2C_{60}$ close to the anode of the external field has negative charge, and the other one has positive charge (see figure 2). The polarization phenomenon makes the single C_{60} and the $2C_{60}$ molecule to be elongated along the electric field direction. When the electric field intensity E_e reaches certain value E_s (called as "saturated field-intensity" here), the above "polarization phenomenon" tends to saturation, i.e. with the further increase of the electric field intensity, the net-charge on each carbon atom tends to saturation. The saturated charges of the atoms close to the anode and cathode are $+4$ and -4 electronic charge per atom, respectively (see figures 2 and 6). The E_s values of the C_{60} and $2C_{60}$ molecule are listed in table 1.

(4) Under the x-, y- and z-axis electric field, all the bridging C–C bonds of the $2C_{60}$ molecule are elongated, see the $l/l_0 - E_e$ curves in figure 7, but the bridging C–C bonds are not observed to break up all the while. Here, the l is the length of the bridging C–C bonds. However, the mechanism of the $2C_{60}$ under the x-axis electric field is different from those under the y- and z-axis field. Under the x-axis electric field, the bridging C–C bonds are elongated along the electric field direction due to the polarization (see figure 2), but, under the y- and z-axis electric field, the elongation of the bridging C–C bonds mainly results from the following reasons: due to the molecular polarization, Regions 1 and 2 of the $2C_{60}$ molecule take positive charge (see figure 6(c)), Regions 3 and 4 negative charge, Regions 1 and 2 exclude each other, Regions 3 and 4 exclude each other too, and the repulsive forces elongate the bridging C–C bonds.

(5) The geometrical deformation, failure behavior, maximal elongation $(d/d_0)_{max}$, critical field-intensity E_c and saturated field-intensity E_s of the $2C_{60}$ molecule under the x-axis field are significantly different from those under the y- and z-axis field (see figures 2–7 and table 1), but the geometrical

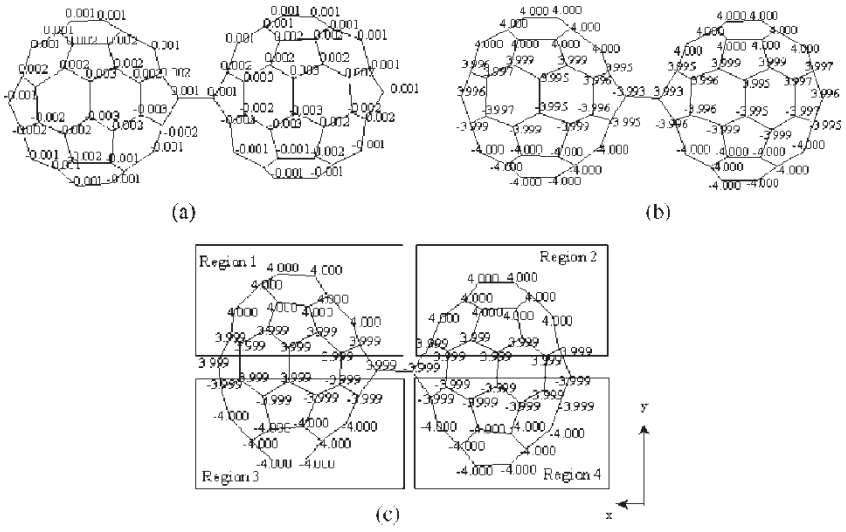

Figure 6. The $2C_{60}$ molecule under the y-axis electric field with the intensity of: (a) 0.025 au, (b) 0.05 au and (c) 0.1 au. (The electric field direction: ↑).

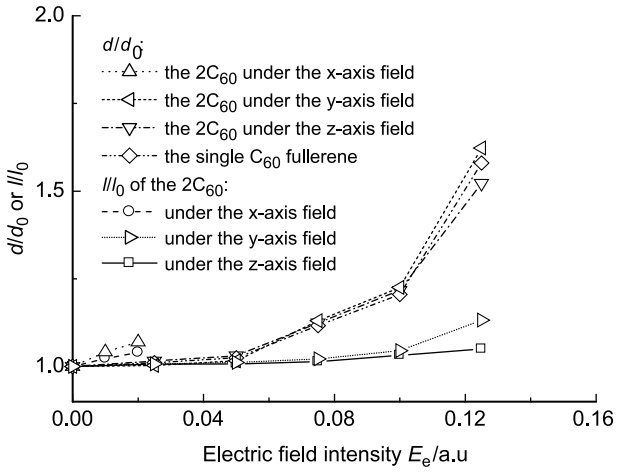

Figure 7. The deformation of the C_{60} and $2C_{60}$ under the electric field.

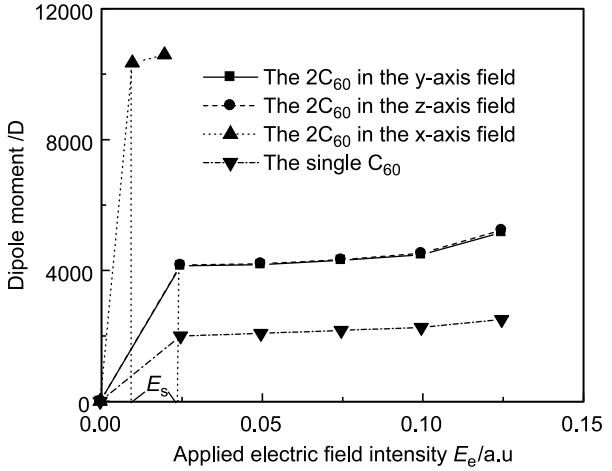

Figure 8. The change of the dipole moment for the C_{60} and $2C_{60}$ molecule with the electric field intensity E_e.

deformation, failure behavior, $(d/d_0)_{max}$, E_c and E_s of the $2C_{60}$ molecule under the *y*- and *z*-axis field are comparatively close to those of the single C_{60} fullerene.

For further investigation of the geometrical evolvement and failure behavior of the $2C_{60}$ molecule under the *x*-axis electric field, figure 8 still presents the change of the dipole moment for the single C_{60} as well as the $2C_{60}$ molecule with the external electric-field intensity E_e. From figure 8, it can be found that when the E_e reaches the E_s, the dipole moment of the molecules tends to saturation that the saturated dipole moment of the $2C_{60}$ molecule under the *x*-axis electric field is about 2.5–3 times bigger than those under the *y*- and *z*-axis electric field, and the curves of the dipole-moment vs. E_e of the $2C_{60}$ molecule under the *y*- and *z*-axis electric-field are very close. Apparently, the difference in the polarization dipole-moment brings the different geometrical evolvement and failure behavior of the $2C_{60}$ molecule.

According to figures 3–8 and table 1, We have enough reason to believe that the $2C_{60}$ molecule under the *y*- and *z*-axis electric-field has the similar deformation mechanism and they can be regard as the case of two side-by-side C_{60} fullerenes under external electric-field because the $2C_{60}$ molecules under both the *y*- and *z*-axis electric-field have not only just twice dipole-moment of the single C_{60} fullerene under the same electric-field intensity (see figure 8) but the same failure pattern as the single C_{60}.

Additionally, in order to validate the present calculations the semi-empirical AM1 method is also used to simulate the $2C_{60}$ under different electric-field direction. The AM1 results are found to be similar to the PM3 ones.

4. Conclusions

The QMD technique is used to simulate the geometrical deformation and failure behavior of the C_{60} fullerene dimer ($2C_{60}$), as well as the single C_{60} fullerene, under external electric field with different direction and intensity. According to the calculated results, the following conclusions can be obtained:

(1) The $2C_{60}$ molecule has the geometrical configuration and failure behavior sensitive to the electric field direction. When the direction of the applied electric field is parallel to the bridging C–C bonds of the $2C_{60}$ molecule, namely along the present *x*-axis, the $2C_{60}$ fails easily, and have the unusual failure behavior.

(2) When the electric field direction is perpendicular to the bridging C–C bonds, namely along the present *x*- or *z*-axis, the $2C_{60}$ has the same polarization and failure mechanism as the single C_{60} molecule under external electric field.

Table 1. The maximal deformation, critical and polarization saturation field-intensity of the C_{60} and $2C_{60}$ molecule.

	The $2C_{60}$			
	Under the x-axis field	*Under the y-axis field*	*Under the z-axis field*	*The single C_{60}*
Maximal deformation $(d/d_0)_{max}$ (%)	≈ 108	≈ 152	≈ 158	≈ 162
Critical field-intensity E_c/au	≈ 0.021	≈ 0.124	≈ 0.122	≈ 0.123
Saturation field-intensity E_s/au	≈ 0.010	≈ 0.025	≈ 0.024	≈ 0.025

Acknowledgements

This work is supported by the Innovation Foundation of NUAA (Y0507-013).

References

[1] H.W. Kroto, J.R. Heath, S.C. O'Brien, R.F. Curl, R.E. Smalley. C_{60}: buckminsterfullerene. *Nature*, **318**, 162 (1985).
[2] H. Shen. Mechanical characters of compressed C_n and endohedral $M@C_{60}$ fullerene molecules. *Chin. J. Mater. Res.*, **18**(6), 645 (2004).
[3] M.E. Kozlov, K. Yakushi. Optical properties of high-pressure phases of C_{60} fullerene. *J. Phys.: Condens. Matter*, **7**, L209 (1995).
[4] R. Sachidanandam, A.B. Harris. Comment on orientational ordering transition in solid C_{60}. *Phys. Rev. Lett.*, **7**, 1467 (1991).
[5] S. Pekker, G. Oszlanyi, L. Forro. Polymer chains in $Rb@C_{60}$ and $K@C_{60}$. *Nature*, **370**, 636 (1994).
[6] H. Shen. Characters of electronic transmission of Au electrode-compressed C_{20} fullerene–Au electrode systems. *Chin. J. Chem. Phys.*, **17**(6), 717 (2004).
[7] G. Wang, K. Komatsu, Y. Murata, M. Shiro. Synthesis and X-ray structure of dumb-bell-shaped C_{120}. *Nature*, **387**, 583 (1997).
[8] B. Ma, J.E. Riggs, Y. Sun. Photophysical and nonlinear absorptive optical limiting properties of C_{60} fullerene dimer and poly-C_{60} fullerene polymer. *J. Phys. Chem. B*, **102**, 5999 (1998).
[9] Y. Guo, W. Guo. Mechanical and electrostatic properties of carbon nanotubes under tensile loading and electric field. *J. Phys. D: Appl. Phys.*, **36**, 805 (2003).
[10] J.J.P. Stewart. Optimization of parameters for semi-empirical methods. *Method J. Comput. Chem.*, **10**, 209 (1989).
[11] A.R. Leach. *Molecular Modeling*, Addison Wesley Longman Limited, London (1996).
[12] Hyperchem 7 is a registered software product of Hypercube, Inc. Hypercube, Inc. 2001.